Electroabsorption measurements and built-in potentials in amorphous silicon p–i–n solar cells

Lin Jiang,[a] Qi Wang,[b] and E. A. Schiff
Department of Physics, Syracuse University, Syracuse, New York 13244-1130

S. Guha and J. Yang
United Solar Systems Corporation, 1100 West Maple Road, Troy, Michigan 48084

Xunming Deng
Energy Conversion Devices, Inc., 1675 West Maple Road, Troy, Michigan 48084

We present a technique for using modulated electroabsorption measurements to determine the built-in potential in semiconductor heterojunction devices. The technique exploits a simple relationship between the second-harmonic electroabsorption signal and the capacitance of such devices. We apply this technique to hydrogenated amorphous silicon (a-Si:H)-based solar cells incorporating microcrystalline Si p^+ layers. For one set of cells with a conventional plasma-deposited intrinsic (i) layer we obtain a built-in potential of 0.98±0.04 V; for cells with an i layer deposited using strong hydrogen dilution we obtain 1.25±0.04 V. We speculate that interface dipoles between the p^+ and i layers significantly influence the built-in potential. © *1996 American Institute of Physics.* [S0003-6951(96)04246-5]

The internal electric fields of amorphous silicon (a-Si:H)-based p–i–n solar cells are crucial to their operation as photocarrier collectors. The *built-in electrostatic potential* V_{bi} established by these fields is, thus, one of a cell's important device parameters. One promising approach to illustrating and estimating V_{bi} exploits electroabsorption measurements: by measuring the transmittance or reflectance of the cell as a function of an external potential V, an inference of the built-in potential can be made.[1–3]

Some corresponding measurements are presented in Fig. 1. The transmittance T of a cell is modulated by a sinusoidal potential of amplitude δV; the transmittance modulation δT_{1f} in phase with δV is then plotted as a function of the external dc potential V. The excellent linearity reflects the quadratic dependence of electroabsorption upon electric field in noncrystalline materials; δT_{1f} ends up being proportional to $\delta V(V-V_{bi})$. The regression lines through the measurements intersect the horizontal axis near $V=1.0$ V, which is an estimate of the built-in potential of this cell. The slopes of the lines indicate the strength of the electroabsorption effect at each wavelength.

As initially reported by Wang, Schiff, and Hegedus,[2] extensive signal averaging of electroabsorption measurements reveals a systematic dependence of this intercept upon wavelength; the effect is evident in the inset of Fig. 1. Wang *et al.* proposed that this wavelength-dependence is a heterostructure effect, since the p^+ and i layers have differing wavelength dependences to their electroabsorption (see also the electroabsorption measurements of Campbell *et al.*,[3] on electroluminescent organic heterostructure diodes). We confirmed this interpretation by studying a-Si:H n–i–m Schottky barrier diodes, which have no p^+ layer. We found no significant wavelength dependence, which is the expected result given the negligible potential drop in the metal.

This heterostructure effect undermines efforts to measure V_{bi} quantitatively using electroabsorption. In this letter, we report on a procedure that we believe resolves this difficulty for a-Si:H-based solar cells. We apply the procedure to two types of n–i–p solar cells having similar n^+ and p^+ layers, but differing a-Si:H i layers. In the simplest possible picture the built-in potential is determined *only* by the Fermi levels of the n^+ and p^+ layers; our estimate of V_{bi} increased from 0.98 to 1.25 V when the i layer was plasma deposited using strong hydrogen dilution.

We first describe the model we use for electroabsorption in a p–i–n solar cell with a-Si:H n^+ and i layers and a microcrystalline p^+ layer. In the upper portion of Fig. 2 we show a schematic illustration of the amplitude of the sinusoi-
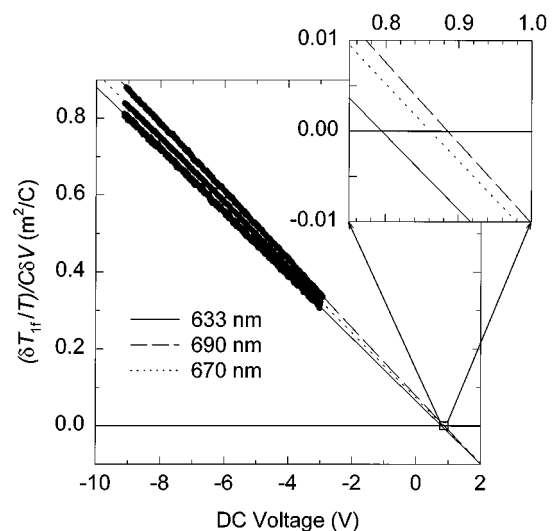

FIG. 1. Modulated electroabsorption signal as a function of the bias potential across the ''standard'' solar cell. Measurements at three laser wavelengths are illustrated; the inset shows that the intercept depends slightly on wavelength.

[a] Electronic mail: Ljiang@mailbox.syr.edu
[b] Present address: National Renewable Energy Laboratory, 1617 Cole Blvd., Golden, CO 80401.

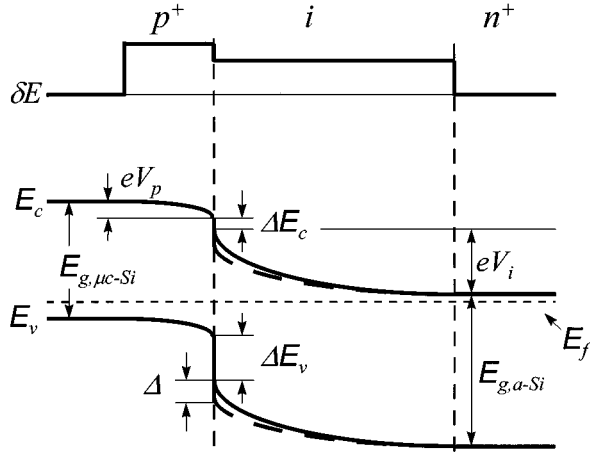FIG. 2. δE is the amplitude of the modulated electric field across a $p-i-n$ solar cell with a microcrystalline p^+ layer. The lower portion indicates the conduction and valence band edges E_c and E_v across the cell, including band bending in the p^+ and i layers, band offsets, and an interface dipole Δ.
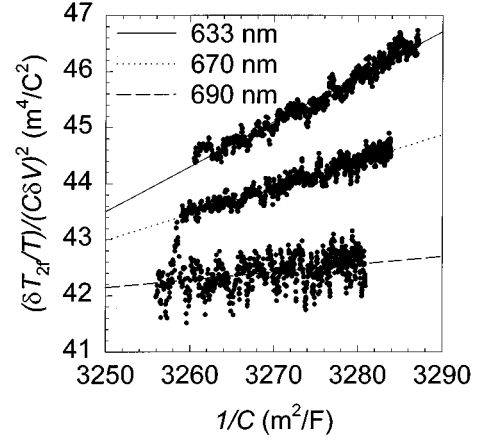

FIG. 3. Plot of the normalized, second-harmonic electroabsorption signal δT_{2f} as a function of reciprocal capacitance for three different wavelengths in the standard cell; the data are generated by varying the reverse bias across the cell.

dally modulated electric field δE. As illustrated, we assumed that this modulation field is uniform across the i layer, and that it extends only across a depletion zone of the p^+ layer. We also simplified the analysis by neglecting potential drops within the n^+ layer of the cell.

The lower portion of Fig. 2 illustrates the steady-state profile of the conduction band and valence band edges E_c and E_v; only the solid black curves are important at present. Figure 2 indicates the band-bending eV_p and eV_i in the p^+ and i layers, respectively. The built-in potential is defined as $V_{bi}=V_p+V_i$. We discuss further details of Fig. 2 subsequently.

The electric field dependent absorption in disordered materials is typically quadratic in field $\alpha(\lambda,E)=\alpha^0(\lambda)+\alpha''(\lambda)E^2$; α'' is the *electroabsorption coefficient* of the material. For a sinusoidal modulation of amplitude δV, there will be corresponding transmittance modulations δT_{1f} and δT_{2f} at the fundamental and the second harmonic of the modulation frequency, respectively. We measure these signals as a function of a reverse bias potential V across the cell. Reverse biasing the cell also increases the width of the depletion zone within the p^+ layer, leading to a decrease in the capacitance $C(V)$ of the cell.

The electroabsorption signals δT_{1f} and δT_{2f} can be obtained from analysis of this model; the derivations are given elsewhere.[4] The second-harmonic signal is particularly important in the present, two-layer system:

$$\frac{\delta T_{2f}/T}{[C(V)\delta V]^2} = \frac{[\alpha_p''(\lambda)/\epsilon_p]}{2\epsilon_0 C(V)} + \frac{[\alpha_i''(\lambda)/\epsilon_i - \alpha_p''(\lambda)/\epsilon_p]}{2\epsilon_0(\epsilon_i\epsilon_0/d_i)} ,$$
$$(1)$$

where d_i is the thickness of the cell's i layers; ϵ_i and ϵ_p are the dielectric constants of the i and p^+ layers, respectively. $C(V)$ refers to the area-normalized capacitance measured at the fundamental modulation frequency. Note that a linear regression of the normalized second-harmonic signal against the reciprocal capacitance of the cell yields electroabsorption properties of *both* the p^+ layer (α_p''/ϵ_p) and of the i layer (α_i''/ϵ_i).

Once these coefficients are known, the built-in potential in the cell can be obtained using the following expression for the normalized fundamental signal:

$$\frac{\delta T_{1f}/T}{C(V)\delta V} = -\frac{2\alpha_i''(\lambda)}{\epsilon_i\epsilon_0}\left\{(V-V_{bi})+V_p\left(\frac{\alpha_p''(\lambda)/\epsilon_p}{\alpha_i''(\lambda)/\epsilon_i}-1\right)\right\}.$$
$$(2)$$

We neglect thin-film interference effects as well as the electric-field dependent refractive index of the films; we do not believe that incorporation of these corrections would significantly alter our conclusions.

In the present work we present measurements on two cells deposited in the sequence $n-i-p$. One cell (denoted ''standard'') has a conventional plasma-deposited a-Si:H i layer; the other (denoted ''strong H dilution'') has an i layer deposited using substantial hydrogen dilution of the silane feedstock gas. Both cells have a-Si:H n^+ layers and ''microcrystalline'' (μc-Si:H) p^+ layers.[5] The open-circuit voltage under AM1.5 illumination were 0.93 V (standard cell) and 1.02 V (strong H dilution) for the as-deposited state.

In Fig. 3 we have shown the measurements of the second-harmonic electroabsorption modulation as a function of capacitance. The data are generated using the same 50 kHz fundamental modulation frequency and reverse bias range as for Fig. 1. The parameter ratios α_p''/ϵ_p and α_p''/ϵ_i are obtained as linear regression parameters from Eq. (1); the results for both types of cell are shown in Fig. 4.

The standard and strongly hydrogen-diluted cells yield quite different spectra α_i''/ϵ_i for the i layers. The results on the standard i layer agree reasonably well with prior work on a-Si:H.[1,2] The results for the hydrogen-diluted i layer presumably reflect the increased band gap for this layer. The electroabsorption spectra of the microcrystalline p^+ layers are similar, which is reasonable since the microcrystalline layers are nominally identical in the two cells. It is reassuring that the very different, raw electroabsorption measurements give this result.

We estimated the built-in potentials in these two cells using the following procedure. We first plotted $(\delta T_{1f}/T)/[C(V)\delta V]$ as a function of bias voltage in order to
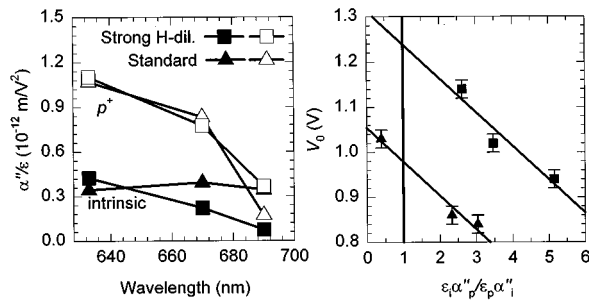
FIG. 4. (*left*) Electroabsorption coefficients α_i'' and α_p'' as a function of wavelength for a-Si:H and for μc-Si:H:B as obtained in cells with standard and with strongly H-diluted i layers. (*right*) Plot of the voltage–axis intercepts V_0 of electroabsorption measurements at three wavelengths vs the corresponding ratios $(\alpha_p''/\epsilon_p)/(\alpha_i''/\epsilon_i)$. The built-in potential V_{bi} is the value of V_0 for $(\alpha_p''/\epsilon_p)/(\alpha_i''/\epsilon_i)=1$ (cf. vertical line).

obtain the voltage–axis intercept V_0. Representative measurements were presented in Fig. 1. V_0 depends slightly upon laser intensity, most likely due to photocharge stored in the samples. In Fig. 4, we have plotted V_0 for low intensities parametrically against the wavelenght-dependent ratio $(\alpha_p''/\epsilon_p)/(\alpha_i''/\epsilon_i)$ (as obtained from Fig. 4). When this ratio is unity, the electroabsorption properties of the p^+ and i layers are the same. As a consequence, the value of the intercept interpolated for this value can be associated with the built-in potential (by the straightforward single-layer analysis). This qualitative argument is confirmed by Eq. (2).

As indicated in Fig. 4, we find $V_{bi}=0.98$ V for the cell with the standard i layer, and $V_{bi}=1.25$ V for the cell with the strong hydrogen dilution intrinsic. The increase in V_{bi} for the strong-hydrogen dilution cell was surprising to us; it is often assumed that the built-in potential in $p-i-n$ diodes is determined by the Fermi levels of the n^+ and p^+ layers only, and is unaffected by the i layer between them.

This argument neglects interfaces, and we speculate that there is a significant *interface dipole* between the p^+ and i layers of a-Si:H-based solar cells. Such dipoles consist of compensating positive and negative electric charges separated by a distance comparable to the carriers' tunneling radii. We illustrated the effect of an interface dipole Δ in Fig. 2. The solid curves represent the band bending without the dipole, and shows the effects of the conduction and valence band offsets ΔE_c and ΔE_v between the p^+ and i layer materials. The dashed curves include an interface dipole that reduces the band bending and, hence, V_{bi}, increasing the apparent size of both band offsets.

The microscopic nature of such interface dipoles is mysterious, although they have been invoked for nearly 50 years in the context of the built-in potentials in Schottky barrier diodes on crystalline semiconductors[6] and are included in textbook treatments of solar cell device physics.[7] For the cells we have studied, it may be that a decrease in interface dipoles for the strongly H-diluted cell is the primary cause for the increase of about 0.1 V in its open-circuit voltage V_{OC} *vis-à-vis* the standard cell; the possibility is an alternative to attributing the increase in V_{OC} to an increase in the energy gap of the i layer.

[1] S. Nonomura, H. Okamoto, and Y. Hamakawa, Appl. Phys. A **32**, 31 (1983).

[2] Q. Wang, E. A. Schiff, and S. S. Hegedus, in *Amorphous Silicon Technology-1994*, edited by E. A. Schiff, M. Hack, A. Madan, M. Powell, and A. Matsuda (Materials Research Society, Pittsburgh, 1994), Vol. 336, p. 365.

[3] I. H. Campbell, M. D. Jowick, and I. D. Parker, Appl. Phys. Lett. **67**, 3171 (1995).

[4] L. Jiang and E. A. Schiff, in *Amorphous Silicon Technology-1996*, edited by M. Hack, E. A. Schiff, S. Wagner, A. Matsuda, and R. Schropp (Materials Research Society, Pittsburgh, in press), Vol. 420.

[5] S. Guha, J. Yang, P. Nath, and M. Hack, Appl. Phys. Lett. **49**, 218 (1986).

[6] E. H. Rhoderick, *Metal-semiconductor Contacts* (Oxford, New York, 1988).

[7] S. J. Fonash, *Solar Cell Device Physics* (Academic, New York, 1981).

Appl. Phys. Lett., Vol. 69, No. 20, 11 November 1996

Jiang *et al.* 3065